catalysts

MDPI

Article

Electrochemical Studies of Pd-Based Anode Catalysts in Alkaline Medium for Direct Glycerol Fuel Cells

Lutho Klaas [1], Mmalewane Modibedi [2], Mkhulu Mathe [2], Huaneng Su [3] and Lindiwe Khotseng [1,*]

1 Faculty of Natural Science, University of the Western Cape, Private Bag X17, Bellville, Cape Town 7535, South Africa; klaasido@gmail.com
2 Energy Materials, Energy Centre, Council for Scientific and Industrial Research, P.O. Box 395, Pretoria 0001, South Africa; mmodibedi@csir.co.za (M.M.); KMathe@csir.co.za (M.M.)
3 Institute of Energy Research, Jiangsu University, 301 Xuefu Road, Zhenjiang 212013, Jiangsu, China; suhuaneng@foxmail.com
* Correspondence: lkhotseng@uwc.ac.za

Received: 25 March 2020; Accepted: 5 June 2020; Published: 26 August 2020

Abstract: This study investigates the most effective electrocatalyst for glycerol oxidation reaction (GOR) in alkaline medium for five synthesized electrocatalysts, Pd, PdNi, PdNiO, $PdMn_3O_4$ and $PdMn_3O_4NiO$, supported on multi-walled carbon nanotubes (MWCNTs) prepared using the polyol method. The particle size and crystalline size of the electrocatalysts were determined using HR-TEM and XRD techniques, respectively, while EDS was used to determine the elemental composition. XRD showed crystalline sizes ranging from 3.4 to 10.1 nm, while HR-TEM revealed particle sizes within the range of 3.4 and 7.2 nm. The electroactivity, electron kinetics and stability of the electrocatalysts towards glycerol in alkaline medium was evaluated using linear sweep voltammetry (LSV), electrochemical impedance spectroscopy (EIS) and chronoamperometry (CA), respectively, while the electroactive surface area (ECSA) of the electrocatalysts was determined using cyclic voltammetry (CV). The metal oxide-based Pd electrocatalysts PdNiO and $PdMn_3O_4$ were the most electrochemically active, while the addition of the second metal oxide to the Pd electrocatalyst $PdMn_3O_4NiO$ did not show any improvement. This was associated with this electrocatalyst having the highest particle and crystalline sizes.

Keywords: glycerol oxidation; electrocatalysts; multi-walled carbon nanotubes; metal oxides

1. Introduction

Liquid fuels (ethanol, glycerol, ethylene glycol) among others have been researched as fuels for low-temperature fuel cells, because of their non-toxic green fuel that is readily produced from renewable resources. Glycerol was selected in this study because the developing amount of biodiesel created worldwide has prompted over two million tons of glycerol to enter the market yearly, consequently making it accessible to a great extent [1]. Glycerol is a polyol alcohol that displays energy densities that are generally practically identical to that of gasoline. Electrochemical oxidation of glycerol has already been considered in the past, and exceptional consideration was given towards the choice of catalyst in alkaline and acid medium [2].

Pt and Pt-based electrocatalysts have been substantially considered for alcohol oxidation due to their effective electro-activity [3–5], but the cost of Pt and the presence of CO as an intermediate during the oxidation of alcohols on Pt-based electrocatalysts leading to the decrease in electrocatalytic activity has severely limited their use [6,7]. This had prompted the advancement of different electrocatalysts, for example, Pd, Ni, Ag, and perovskite-type oxides, to improve the oxidation

of alcohols. Among them, Pd and Pd-based materials are favourable electrocatalysts for the oxidation of alcohols. They could potentially be used for alkaline direct alcohol fuel cells as they present high electrocatalytic activity compared to acid direct alcohol fuel cell technology that uses platinum-based electrocatalysts [8–10]. Pd-based electrocatalysts continue to be considered due to their excellent properties within alcohol electrocatalytic oxidation in alkaline solution, in contrast to Pt electrocatalysts [11,12]. Another advantage is that the electrode does not suffer severely from poisoning in an alkaline solution more than in acid, since bonding of the chemisorbed intermediates on the catalyst is weak and also the recommended harming amount of the suggested poisoning species CO_{ads} is smaller than in an acidic solution [13].

Much work on the improvement of novel Pd-based catalysts for the oxidation of alcohols has been executed. Normally, nanosized Pd electrocatalysts display improved electroactivity for the oxidation of alcohols with the addition of another metal to the Pd, increasing its electrocatalytic activity. The catalyst support affects the exhibition of the catalysts and the catalyst layer [14]. The utilization of high surface area carbon materials, for example, activated carbon, carbon nanofibers and carbon nanotubes as new electrode materials, has been considered by fuel cell investigators because of their improved physical-chemical properties and good corrosion resistance [14]. In particular, carbon nanotubes have been recently recommended as the favourable supports for fuel cell catalysts because of their excellent attributes, which include high perspective ratio, high electron conductivity and high mass transport capability [10,15]. Pd nanoparticles with sizes 4–30 nm have been acquired by the unconstrained decrease of Pd^{2+} on the multi-walled carbon nanotubes as the prepared Pd electrocatalysts demonstrate enhanced electrocatalytic properties for alcohol oxidation [15].

There are various types of synthesis methods for electrocatalysts including impregnation, polyol and micro-emulsion methods. The preparation methods influence the mean particle size, particle size distribution, distribution of catalyst crystal surfaces and catalyst morphology, amongst other things, hence the electrocatalytic activity of the metal catalysts [16,17]. A huge advantage of the polyol method is the low operating temperatures, where the process is able to control properties of the particles such as size, shape and uniformity. In this paper, we report glycerol electro-oxidation on Pd, PdNi, PdNiO, $PdMn_3O_4$ and $PdMn_3O_4NiO$ supported on functionalized multi-walled carbon nanotubes (MWCNT). The catalysts were synthesized using the polyol technique, with sodium borohydride as the reducing agent, and structurally characterized using X-ray diffraction (XRD), electron diffraction spectroscopy (EDS), and high-resolution transmission electron microscopy (HR-TEM). The electrochemical measurements were executed in a three-electrode glass cell to evaluate the electrocatalytic activity of the different materials for glycerol electro-oxidation and the highest electrochemically active electrocatalyst using cyclic voltammetry; electrochemical impedance spectroscopy and chronoamperometry were utilized to determine the electrode kinetics and stability of the prepared catalysts, respectively.

2. Results and Discussion

2.1. Structural Characterization of Pd/MWCNT, PdNi/MWCNT, PdNiO/MWCNT, $PdMn_3O_4$/MWCNT and $PdMn_3O_4NiO$/MWCNT Electrocatalysts

Energy-dispersive X-ray spectroscopy (EDS) was utilized to determine the metal loading of the electrocatalysts. The prepared electrocatalysts results show that the monometallic Pd has a wt.% of 19.38, while the binary catalysts have a Pd wt.% in the range of 16 with the second metal in the range between 5 to 7 wt.%. For the ternary catalyst, the Pd has a wt.% of 13.89 with the other two metals in the range of 4.26 and 5.65 wt.%. The ratio for the binary catalysts is (1:1), while for the ternary catalysts it is (1:1:2). The composition of all the catalysts is given in Table 1. All catalysts present atomic ratios that are comparable; the information about the microstructure of the prepared electrocatalysts was determined using HR-TEM and XRD.

Table 1. Nominal weight percentages obtained using energy-dispersive X-ray spectroscopy (EDS), particle sizes obtained using high-resolution transmission electron microscopy (HR-TEM) and crystallite sizes calculated using Scherrer's equation of the electrocatalysts.

Pd Atomic Ratio (Nominal)	Pd Atomic Ratio-EDS			Particle Size (nm) TEM	Crystallite Size (nm) XRD
	Pd	Ni	Mn		
Pd/MWCNT	19.38	-	-	5.2	5.2
PdNi/MWCNT	16.25	5.25	-	5.1	4.0
PdNiO/MWCNT	16.03	6.23	-	3.4	3.4
$PdMn_3O_4$/MWCNT	15.47	-	7.25	5.3	6.5
$PdMn_3O_4NiO$/MWCNT	13.89	4.26	5.65	7.2	10.1

XRD measurements were conducted to attain the crystallographic data of the prepared electrocatalysts. The XRD patterns for the prepared electrocatalysts are shown in Figure 1 below. The diffraction peak for carbon attributed by the MWCNTs at about 2θ = 25°, which corresponds to (002), is one of the five major peaks including the four from Pd. The strongest and sharpest diffraction peak for all five electrocatalysts is around 2θ = 40.05°, which could be indexed as (111) reflection of Pd, and the other trademark Pd diffraction peaks at 2θ of about 47.05°, 67.95° and 82.10° corresponded to (200), (220) and (310), respectively [1]. The XRD results indicate that these peaks are characteristic of the face-centred cubic (fcc) structure of Pd [18]. The diffraction peaks were completely seen at the equivalent 2θ values for all the prepared catalysts showing no significant peak shift, showing the Pd and the metal oxides did not alloy. The XRD patterns for PdNiO, $PdMn_3O_4$ and $PdMn_3O_4NiO$ on MWCNT support show the peaks for the Pd structure and the diffraction peaks for the metal oxides indicating that they coexist in the sample. The crystalline size of the electrocatalysts is determined based on the broadening of the (220) diffraction peak according to Scherrer's equation [19]. From Table 1 the average particle size can be seen with PdNiO, showing the smallest crystallite size of 3.37 nm.

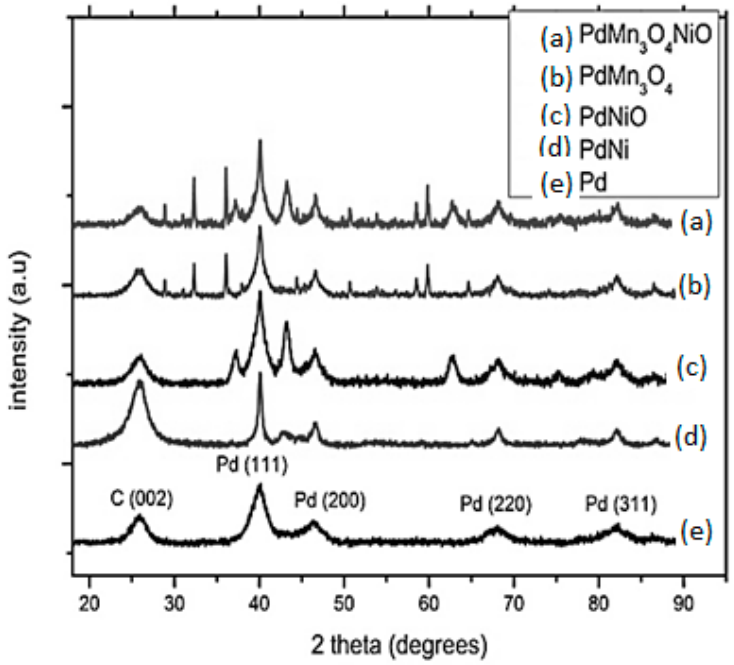

Figure 1. X-ray diffractograms of Pd, PdNi, PdNiO, $PdMn_3O_4$ and $PdMn_3O_4NiO$ electrocatalysts on MWCNT support.

Figure 2 is the TEM micrographs of Pd, PdNi, PdNiO, $PdMn_3O_4$ and $PdMn_3O_4NiO$ electrocatalysts on MWCNT. The cylinder-like particles are multi-walled carbon nanotube (MWCNT) supports, with a thickness of about 20 nm. The little dark dots are the electrocatalyst nanoparticles. The TEM

micrographs of the prepared electrocatalysts present agglomeration of the nanoparticles on the carbon support. Such characteristics decrease the surface area required for fuel adsorption, hence decreasing the electrocatalyst activities. When comparing the electrocatalysts, the PdNi/MWCNT and PdNiO/MWCNT have the least agglomeration. The particle size was determined using Image J software, and the two least agglomerated catalysts gave the smallest particle sizes. The PdNiO showed the smallest particle of 3.44 nm; this favours the most electrocatalytic activity towards alcohol oxidation. The other electrocatalysts, Pd, PdNi, $PdMn_3O_4$ and $PdMn_3O_4NiO$, on MWCNT support had a particle size of between 4.01 and 10.06 nm. The particle sizes acquired using HR-TEM were comparable with the average particle sizes obtained using XRD following the order $PdMn_3O_4NiO$/MWCNT > $PdMn_3O_4$/MWCNT> Pd/MWCNT > PdNi/MWCNT > PdNiO/MWCNT.

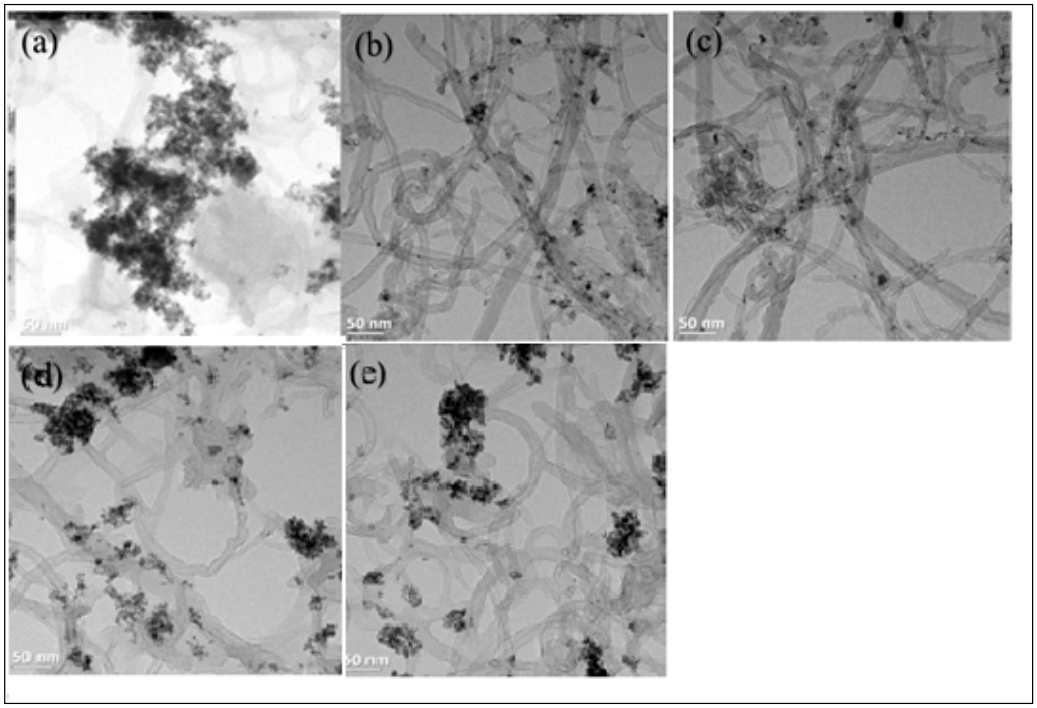

Figure 2. HR-TEM micrographs of (**a**) Pd, (**b**) PdNi, (**c**) PdNiO, (**d**) $PdMn_3O_4$ and (**e**) $PdMn_3O_4NiO$ electrocatalysts on MWCNT.

2.2. *Evaluation of Electrocatalytic Activity for Pd/MWCNT, PdNi/MWCNT, PdNiO/MWCNT, $PdMn_3O_4$/MWCNT and $PdMn_3O_4NiO$/MWCNT Electrocatalyst in Alkaline Solution*

Electrochemical characteristics of the prepared electrocatalysts in 1 M KOH solution were primarily analysed using cyclic voltammetry, as shown in Figure 3. From the cyclic voltammetry of the prepared electrocatalysts, the oxidation and reduction peaks for the different electrocatalysts are observed. The oxidation peak for all the prepared electrocatalysts is observed at ca. −0.3 V, except for $PdMn_3O_4$ with the most intense peak at ca. −0.12 V. While the reduction peak is attributed to the reduction of the Pd oxides produced, on the forward potential scan it is observed between ca. −0.3 V to −0.4 V, with $PdMn_3O_4$ being the most intense, indicating that it would possess the largest real surface area [10]. The peak area of the reduction peak of the electrocatalysts in the cyclic voltammetry was used to determine the electroactive surface area of the catalysts using the equation [20]:

$$ECSA\left(\mathrm{cm}^2/\mathrm{g}\right) = \frac{Q\left(C/\mathrm{cm}^2\right)}{420\ \mu\mathrm{C}/\mathrm{cm}^2.l\ \left(\mathrm{g}/\mathrm{cm}^2\right)}$$

where Q is the charge from the reduction peak of catalyst in Coulomb, l is the working electrode catalyst loading in $g{\cdot}cm^{-2}$, and 420 μCcm^{-2} is the value for the oxygen monolayer of Pd [21]. The obtained

electroactive surface area (ECSA) values are 61.45 m^2/g for $PdMn_3O_4$/MWCNT, 31.39 m^2/g for PdNiO/MWCNT, 27.11 m^2/g for $PdMn_3O_4$NiO/MWCNT, 16.29 m^2/g for PdNi/MWCNT and 14.43 m^2/g for Pd/MWCNT. Adding the second metal oxide to the Pd did not contribute as it ended up with the lowest ECSA value, which can be attributed to its high particle size values hence lower surface area compared to the other catalysts. The high ECSA value for binary Pd-based electrocatalysts can be attributed to their lower particle sizes and electrochemical reaction kinetics [16].

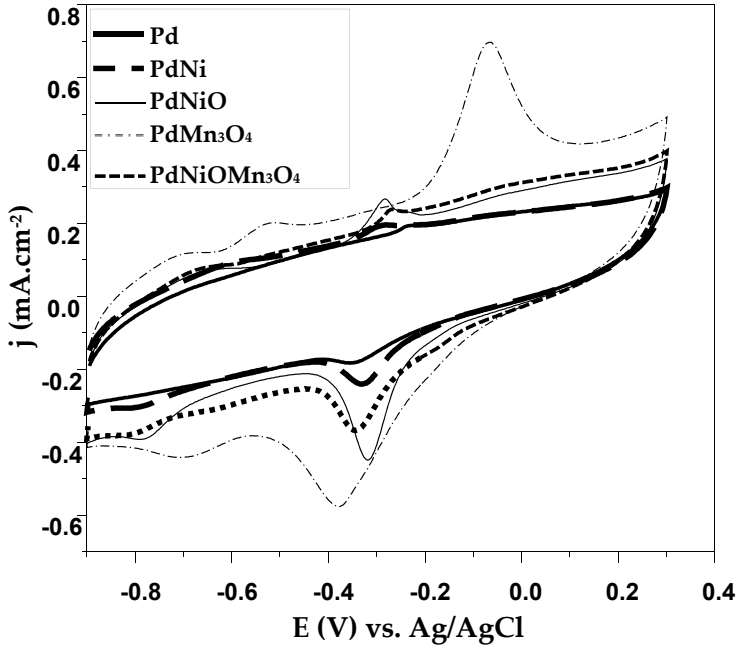

Figure 3. Cyclic voltammetry of Pd, PdNi, PdNiO, $PdMn_3O_4$ and $PdMn_3O_4$NiO electrocatalysts on MWCNT support in N_2 saturated 1.0 M KOH at a scan rate of 30 mVs^{-1}.

2.3. Comparison of Glycerol Oxidation on Pd/MWCNT, PdNi/MWCNT, PdNiO/MWCT, $PdMn_3O_4$ and $PdMn_3O_4$NiO/MWCNT Electrolytes in KOH Solution

The electrocatalytic activities of the prepared electrocatalysts for glycerol electro-oxidation in alkaline solution were explored using linear sweep voltammetry, shown in Figure 4. From the figure it is observed that all the metal oxide-based Pd electrocatalysts show the best electrocatalytic activity with higher current density towards glycerol oxidation following the order PdNiO/MWCNT > $PdMn_3O_4$NiO/MWCNT > $PdMn_3O_4$/MWCNT > PdNi/MWCNT > Pd/MWCNT, confirming that metal oxide-supported electrocatalysts are more electroactive than metal-supported electrocatalysts [22]. The superior glycerol oxidation reaction (GOR) catalytic activity of the prepared electrocatalysts was determined using current density based on ECSA. The PdNiO/MWCNT with the smallest particle size exhibits the highest catalytic activity, 0.84 A/g, following the trend of $PdMn_3O_4$NiO/MWCNT with 0.71 A/g, $PdMn_3O_4$/MWCNT and PdNi/MWCNT with 0.69 A/g and Pd/MWCNT with 0.60 A/g [23]. The same trend was obtained by Shen et al. under ethanol electro-oxidation [24]. In addition, the on-set potential was mostly negative for $PdMn_3O_4$/MWCNT (−0.48 V) followed by $PdMn_3O_4$NiO/MWCNT (−0.39 V), PdNiO/MWCNT (−0.36 V) and PdNi/MWCNT (−0.35 V), respectively compared to Pd/MWCNT, with on-set potential at −0.25 V. [25].

Electrochemical impedance spectroscopy (EIS) was utilized to explore the catalytic kinetics regarding the glycerol electrochemical oxidation [26,27]. Electrochemical impedance spectroscopy is one of the most effective techniques used to explore the electrochemical parameters of the electrode/electrolyte interface [28]. Figure 5 shows the interfacial behaviour of the prepared catalysts in KOH electrolyte containing glycerol at the potential of −0.3 V vs. Ag/AgCl tested at a frequency range of 0.01 to 10^5 Hz. An equivalent circuit was utilized for fitting the Nyquist plots (insert),

which includes Rs (solution resistance), Rct (charge transfer resistance), Qdl (double-layer capacitance) and Zw (Warburg resistance). Warburg impedance is due to a mass transfer resistance for the redox reaction during diffusion from and to the electrode surface [29].

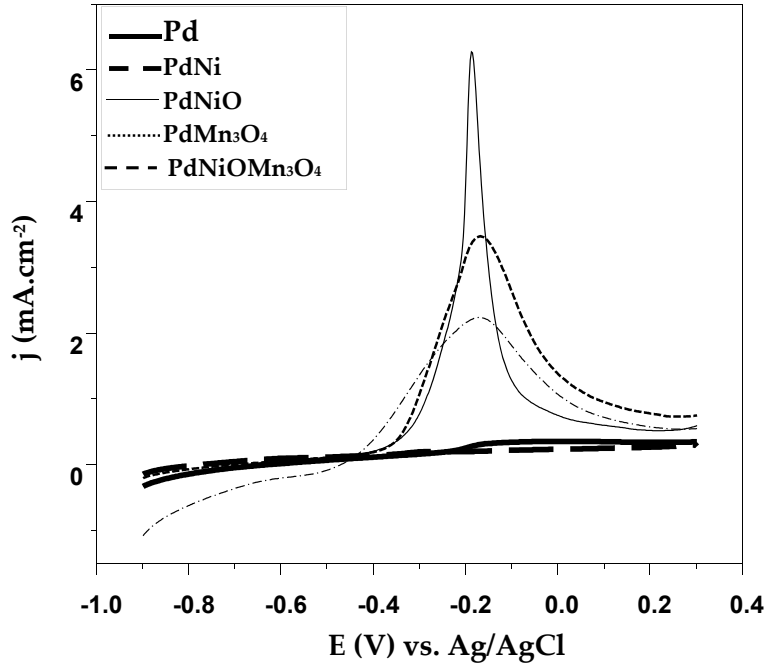

Figure 4. Linear sweep voltammetry of Pd, PdNi, PdNiO, $PdMn_3O_4$ and $PdMn_3O_4NiO$ electrocatalysts on MWCNT support in N_2 saturated 1.0 M KOH with 1.0 M glycerol at a scan rate of 30 $mV{\cdot}s^{-1}$.

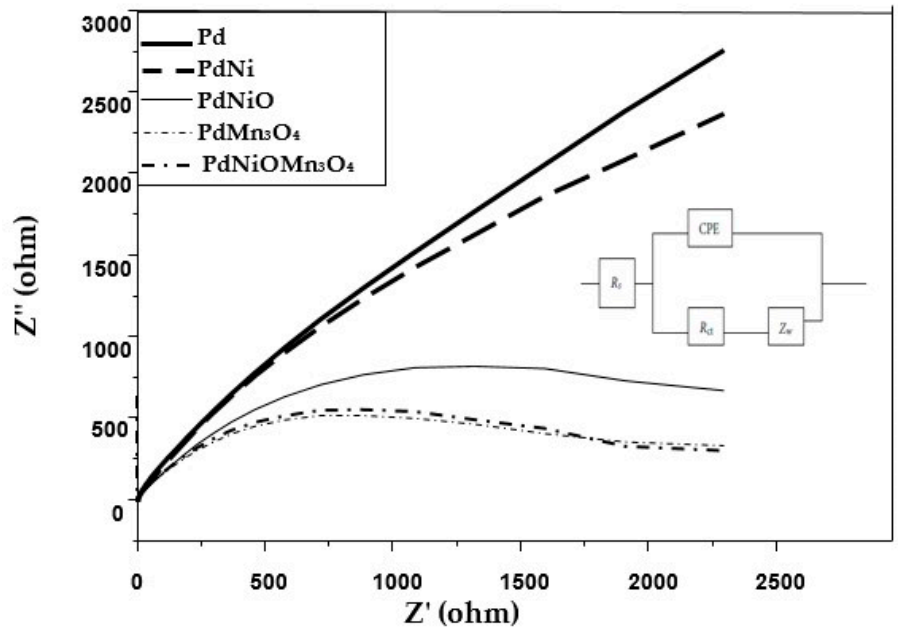

Figure 5. Nyquist plots for Pd, PdNi, PdNiO, $PdMn_3O_4$ and $PdMn_3O_4NiO$ electrocatalysts on MWCNT support in N_2 saturated 1.0 M KOH and 1.0 M glycerol under potential −0.3 V vs. Ag/AgCl. Insert: proposed equivalent circuit.

Typically, each plot shows a semicircle in the high frequency related to the charge transfer. The Rct value of Pd decreases with the addition of a second metal Ni and decreases even further when the metal oxides are added. The results indicate that the addition of metal oxides significantly

improves the charge transfer kinetics of Pd catalysts and encourages mass transfer. The Rct values calculated using Randel's cell fitting were 309 Ωcm^2 and 196 Ωcm^2 for Pd/MWCNT and PdNi/MWCNT electrocatalysts and 136.3 Ωcm^2, 40.3 Ωcm^2 and 42.3 Ωcm^2 for PdNiO/MWCNT, $PdMn_3O_4$/MWCNT and $PdMn_3O_4$NiO/MWCNT under open circuit, respectively.

As expected, the charge transfer resistance of metal oxide-based electrocatalysts decreased, hence the slow reaction rate of glycerol dehydrogenation for Pd/MWCNT and PdNi/MWCNT electrocatalysts compared to PdNiO/MWCNT, $PdMn_3O_4$/MWCNT and $PdMn_3O_4$NiO/MWCNT [30]. The electrochemical reaction kinetics is in agreement with the ECSA, with Pd-based metal oxide catalysts having the highest ECSA values compared to Pd and PdNi, all on MWCNT support.

The catalytic stability of electrocatalysts is very important for their real applications in direct alcohol fuel cells (DAFCs) [29]. Figure 6 shows chronoamperometry (CA) of Pd, PdNi, PdNiO, $PdMn_3O_4$ and $PdMn_3O_4$NiO electrocatalysts on MWCNT support in N_2 saturated 1.0 M KOH with 1.0 M glycerol at −0.2 V [29]. This was to test the catalytic stability of the different catalysts towards glycerol oxidation [31–35] after 1800 s. In chronoamperometry (CA), it was observed that the current density reduced abruptly for about the first 100 s. It is known that, toward the start, the current density in CA measurements declines sharply with time (I proportional to $t^{-1/2}$). The diminishing rate with time may portray the harming of the electrodes by the results of the glycerol oxidation reaction [18]. When comparing the prepared catalysts, as observed in Figure 6, the Pd catalyst with metal oxides performed better than the other catalysts, with $PdMn_3O_4$ being the one with the highest steady current density, indicating slight performance degradation [34], followed by $PdMn_3O_4$NiO and PdNiO, all on MWCNT support (as seen from the insert). The results obtained correspond to the literature where oxides are expected to increase the stability of Pd-based catalysts when alloyed to them [27,35].

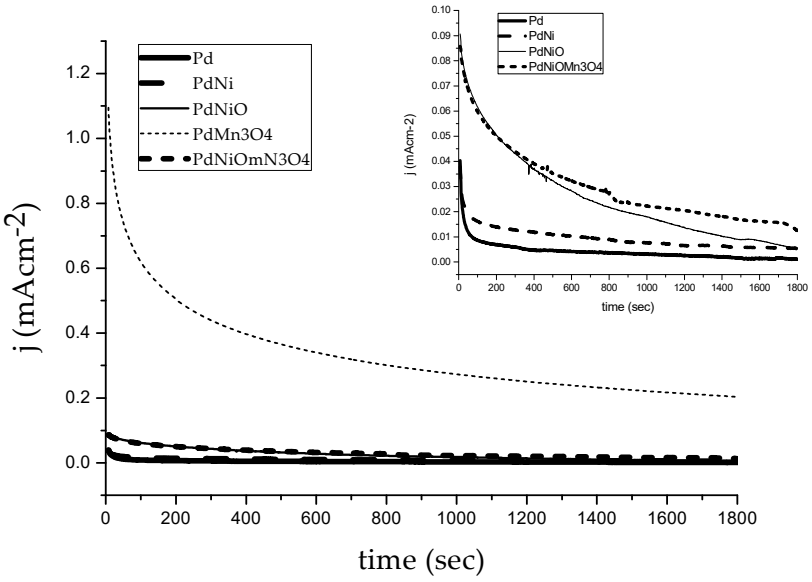

Figure 6. Chronoamperometry of Pd, PdNi, PdNiO, $PdMn_3O_4$ and $PdMn_3O_4$NiO electrocatalysts on MWCNT support in an N_2-saturated solution of 1.0 mol L^{-1} glycerol and 1.0 mol L^{-1} KOH at 25 °C.

3. Materials and Methods

3.1. Materials Used

The chemicals utilized in the preparation were $PdCl_3$ and $NiCl_3$, purchased from 99.5%, Alfa Aesar; Haverhill, MA, USA; NiO, Mn_3O_4 and HCl, purchased from Sigma Aldrich Chemical Co., St. Louis, MI, USA; and ethylene glycol, KOH, C_3H_8O, $C_3H_8O_3$, C_2H_6O, HNO_3 and H_2SO_4, purchased from Kimix Chemical and Lab supplies, cc, Cape Town, WC, South Africa. All the chemicals were utilized as received with no additional treatment. The multi-walled carbon nanotubes (MWCNTs) were bought

from carbon nano-material technology Co. Ltd., Gargdong Gyongju, Gyeonggi, South Korea, with a width of ~20 nm and a length of ~10 μm. Before the MWCNTs were used, they were first oxidized in a hot solution consisting of a mixture of $HNO_3\backslash H_2SO_4$ (Kimix Chemical and Lab supplies, cc., Cape Town, WC, South Africa) (1:3) *v/v*. All synthesis was done using deionized water from the Milli-Q water purification system (Millipore, Bedford, MA, USA).

3.2. Electrocatalyst Preparation

All electrocatalysts were prepared utilizing the polyol technique. To synthesize the PdNi/MWCNT electrocatalysts, 71.2 mg of $PdCl_2$ and 24 mg of $NiCl_2$ was liquefied in the mixture of 48 mL ethylene glycol and 16mL water, under stirring, to attain a homogenous solution. To the above solution, 240 mg of functionalised MWCNT particles were included and sonicated for 30 min. A solution of 2 g $NaBH_4$ liquefied in 48 mL ethylene glycol was gradually added to the mixture under dynamic stirring for 4 h. Then after stirring for 4 h, the mixture was filtered and washed with ultrapure water and then dried overnight in an oven. The same procedure was followed for the preparation of Pd/MWCNT and deposition of Pd electrocatalyst on Mn_3O_4 and NiO.

3.3. Electrocatalyst Evaluation

Electrochemical measurements were done at ambient temperatures utilizing the three-electrode system, which incorporates the working, reference and counter electrodes. A Pt foil was utilized as a counter electrode, and an Ag/AgCl electrode was used as a reference electrode. The working electrode was a glassy carbon disc (5 mm in dimension with a geometric area of 0.196 cm^2) secured with a thin layer of catalyst. All electrochemical tests were done utilizing cyclic voltammetry (CV), linear sweep voltammetry (LSV), electrochemical impedance spectroscopy (EIS) and chronoamperometry (CA) on an Autolab electrochemical workstation (PGSTAT128N, Eco Chemie, Netherlands). CA tests were done at an oxidation potential window from −2.0 V vs. Ag/AgCl for 30 min. CV assessments were measured with the Ohmic resistance error at 30 mV/s, covering a potential window from −1.0 V to 0.8 V vs. Ag/AgCl. 1.0 M potassium hydroxide was used as the electrolyte. For the evaluation of glycerol electro-oxidation, 1.0 M glycerol was added to the electrolyte. Nitrogen was used to deoxygenate the solutions. Before the experiment, the electrode substrate was pre-treated by polishing using alumina, preceded by ultrasonic cleaning in water and afterwards flushed to get a spotless surface. To obtain a homogeneous catalyst layer, a method described by Garsany Y. et al. [20] was used. In the procedure, a mixture of 25 mg of catalyst powder, 20 μL of Nafion, 5 mL of isopropanol and 4.15 mL of ultrapure water was normalized in an ultrasonic bath. A measured amount of this mixture was plunged on top of the glassy carbon disc and then dried to form the desired catalyst layer.

3.4. Physical Characterization

To obtain more details on the catalyst structure, X-ray diffraction (XRD) patterns were executed using a Bruker AXS D8 Advance instrument, (Cramerview, South Africa); Cu-Kα radiation, λ = 1.5406 Å. The Bragg angle array was 2θ = 10–90° with a scanning step of 0.035°. A standard α-Al_2O_3 sample was utilized for the assurance of the instrumental commitment into top profile parameters.

The high-resolution transmission electron microscope (HR-TEM) micrographs were obtained using a JEOL 2010 TEM system (Carl Zeiss, Jena, Germany); operating at 200 kV. The HR-TEM samples were prepared by dispersing the carbon-supported electrocatalysts in ethanol, and then a drop of the suspension was cast onto the carbon-film-covered Cu grid for analysis. The particle size determined using HR-TEM was obtained using Image J software (Image Processing and Analysis in Java developed at the National Institutes of Health and the Laboratory for Optical and Computational Instrumentation, LOCI, University of Wisconsin, Madison, WI, USA) over multiple areas for each electrocatalyst. Energy dispersive X-ray spectroscopy (EDS) coupled to the scanning electron microscopy (JOEL JSM-7500F Scanning Electron Microscope, Mundelein, IL, USA), evaluated the catalyst composition.

4. Conclusions

In summary, this examination expected to investigate new Pt free electrocatalysts in DAFC. From the study, the Pd, PdNi, PdNiO, $PdMn_3O_4$ and $PdMn_3O_4NiO$ supported on MWCNT were successfully fabricated using the polyol method. The synthesized electrocatalysts had particle sizes of 3.4–7.2 nm and average particle sizes of 3.4–10.1 nm, determined using HR-TEM and XRD, respectively. No alloy phase is pronounced for the prepared electrocatalysts according to XRD analysis. It is found that the metal oxide-based electrocatalysts present enhanced electrocatalytic activity towards glycerol oxidation compared to Pd and PdNi on MWCNT support. Furthermore, the PdNiO/MWCNT had the largest current density for glycerol oxidation compared to other electrocatalysts. This can be attributed to it having the smallest particle size and being the most active towards anode oxidation reaction. From the electrochemical impedance spectroscopy, it was concluded that the metal oxide-based Pd electrocatalysts' electrochemical reaction kinetics were faster than those of Pd/MWCNT and PdNi/MWCNT. This can be ascribed to the highest ECSA values for metal oxide-based Pd electrocatalysts compared to Pd and PdNi, all on MWCNT support. $PdMn_3O_4$ is found to be the most stable electrocatalyst followed by $PdNiOMn_3O_4$, PdNiO, PdNi and Pd, respectively, from the chronoamperometry. Based on all the results acquired in the investigation, it was concluded that adding a metal oxide to the electrocatalyst improves its performance.

Author Contributions: All authors have contributed to the research work. Investigation, L.K. (Lutho Klaas), Conceptualization, L.K. (Lindiwe Khotseng) and M.M. (Mmalewane Modibedi); Project administrator, M.M. (Mkhulu Mathe); and funding acquisition, H.S. All authors have read and agreed to the published version of the manuscript.

Funding: This research was funded by National Research Foundation (NRF), South Africa, grant number: 120375 and Tertiary Education Support Program (TESP), Eskom Holdings SOC Limited Reg No 2002/015527/06.

Acknowledgments: We greatly appreciate the Physics Department (UWC) for HR-TEM and EDS analysis and iThemba Labs for XRD analysis.

Conflicts of Interest: The authors declare no conflict of interest. The funders had no role in the design of the study; in the collection, analyses, or interpretation of data; in the writing of the manuscript, or in the decision to publish the results.

References

1. Antolini, E.; Perez, J. Anode catalysts for alkaline direct alcohol fuel cells and characteristics of the catalysts layer. In *Electrocatalysis in Fuel Cells*; Shao, M., Ed.; Springer: London, UK, 2013; pp. 89–127.
2. Pulido, D.F.Q.; Kortenaar, M.V.T.; Hurink, J.L.; Smit, G.J.M. A Practical Approach in Glycerol Oxidation for the Development of A Glycerol Fuel Cell. *Trends Green Chem.* **2017**, *3*, 1–17. [CrossRef]
3. Alvarez, G.F.A.; Mamlouk, M.; Scott, K. An Investigation of Palladium Oxygen Reduction Catalysts for the direct methanol Fuel Cell. *Int. J. Electrochem.* **2011**, *2011*, 684535. [CrossRef]
4. He, Q.; Shyam, B.; Macounova, K.; Krtil, P.; Ramaker, D.; Murajee, S. Dramatically enhanced cleavage of the C–C bond using an electrocatalytically coupled reaction. *J. Am. Chem. Soc.* **2012**, *134*, 8655–8661. [CrossRef] [PubMed]
5. Ribeiro, J.; Dos Anjos, D.M.; Kokoh, K.B.; Coutanceau, C.; Lager, J.-M.; Olivi, P.; de Andrade, A.R.; Tremiliosi-Filho, G. Carbon-supported ternary PtSnIr catalysts for direct ethanol fuel cell. *Electrochim. Acta* **2007**, *52*, 6997–7006. [CrossRef]
6. Xue, X.; Ge, J.; Tian, T.; Liu, C.; Xing, W.; Lu, T. Enhancement of the electrooxidation of ethanol on Pt-Sn-P/C catalysts prepared by chemical deposition process. *J. Power Sources* **2007**, *172*, 560–569. [CrossRef]
7. Jiang, L.; Colmenares, L.; Jusys, Z.; Sun, G.Q.; Behm, R.J. Ethanol electrooxidation on novel carbon supported Pt/SnOx/C catalysts with varied Pt: Sn ratio. *Electrochim. Acta* **2007**, *53*, 377–389. [CrossRef]
8. Geraldes, A.N.; da Silva, D.F.; da Silva, J.C.M.; de Sa, O.A.; Spinace, E.V.; Neto, A.O.; Dos Santos, M.C. Palladium and palladium-tin supported on multi-wall carbon nanotubes or carbon for alkaline direct ethanol fuel cell. *J. Power Sources* **2015**, *275*, 189–199. [CrossRef]

9. Rajalakshmi, N.; Ryu, H.; Shaijumon, M.M.; Ramaprabhu, S. Performance of polymer electrolyte membrane fuel cells with carbon nanotubes as oxygen reduction catalyst support material. *J. Power Sources* **2005**, *140*, 250–257. [CrossRef]
10. Yi, Q.; Chu, H.; Chen, Q.; Yang, Z.; Liu, X. High-performance Pd, PdNi, PdSn and PdSnNi nanocatalysts supported on carbon nanotubes for electrooxidation of C2-C4 alcohols. *Electroanalysis* **2015**, *27*, 388–397. [CrossRef]
11. Waje, M.M.; Li, W.; Chen, Z.; Yan, Y. Durability Investigation of Cup-Stacked Carbon Nanotubes Supported Pt as PEMFC Catalyst. *ECS Trans.* **2006**, *3*, 677–683.
12. Yuan, X.-Z.; Song, C.; Wang, H.; Zhang, J. *Electrochemical Impedance Spectroscopy in PEM Fuel Cells*; Springer: London, UK, 2010; pp. 193–262.
13. Yu, E.H.; Krewer, U.; Scott, K. Principles and Materials Aspects of Direct Alkaline Alcohol Fuel Cells. *Energies* **2010**, *3*, 1499–1528. [CrossRef]
14. Hernandez, R.; Dunning, C. Direct methanol fuel cells. In *Electrocatalysts for Direct Methanol Fuel Cells*; Khotseng, L., Ed.; Nova Science Publishers: New York, NY, USA, 2017; pp. 1–49.
15. Yi, Q.F.; Sun, L.Z. In situ synthesis of palladium nanoparticles on multi-walled carbon nanotubes and their electroactivity for ethanol oxidation. *Rare Met.* **2013**, *32*, 586–591. [CrossRef]
16. Santasalo-Aarnio, A.; Kwon, Y.; Ahlberg, E.; Kontturi, K.; Kallio, T.; Koper, M.T. Comparison of methanol, ethanol and iso-propanol oxidation on Pt and Pd electrodes in alkaline media studied by HPLC. *Electrochem. Commun.* **2011**, *13*, 466–469. [CrossRef]
17. Yougui, C.; Zhuang, L.; Juntao, L.U. Non-Pt Anode Catalysts for Alkaline Direct Alcohol Fuel Cells. *Chin. J. Catal.* **2007**, *28*, 870–874.
18. Wang, R.; Wang, H.; Feng, H.; Ji, S. Palladium Decorated Nickel Nanoparticles Supported on Carbon for Formic Acid Oxidation. *Int. J. Electrochem. Sci.* **2013**, *8*, 6068–6076.
19. Lv, H.; Cheng, N.; Mu, S.; Pan, M. Heat-treated multi-walled carbon nanotubes as durable supports for PEM fuel cell catalysts. *Electrochim. Acta* **2011**, *58*, 736–742. [CrossRef]
20. Garsany, Y.; Baturina, O.A.; Swider-Lyons, K.E.; Kocha, S.S. Experimental methods for quantifying the activity of Platinum electrocatalysts for the oxygen reduction reaction. *Anal. Chem.* **2010**, *82*, 6321–6328. [CrossRef]
21. Łukaszewski, M.; Soszko, M.; Czerwiński, A. Electrochemical Methods of Real Surface Area Determination of Noble Metal Electrodes—An Overview. *Int. J. Electrochem. Sci.* **2016**, *11*, 4442–4469. [CrossRef]
22. Zhao, G.; Yang, F.; Chen, Z.; Liu, Q.; Ji, Y.; Zhang, Y.; Niu, Z.; Mao, J.; Bao, X.; Hu, P.; et al. Metal/oxide interfacial effects on the selective oxidation of primary alcohols. *Nat. Commun.* **2017**, *8*, 1–8. [CrossRef]
23. Lu, X.; Zhao, C. Electrodeposition of hierarchically structured three-dimensional nickel-iron electrodes for efficient oxygen evolution at high current densities. *Nat. Commun.* **2015**, *6*, 6616. [CrossRef]
24. Shen, P.K.; Xu, C. Alcohol oxidation on nanocrystalline oxide Pd/C promoted electrocatalysts. *Electrochem. Commun.* **2006**, *8*, 184–188. [CrossRef]
25. Pohl, M.D.; Watzele, S.; Calle-Vallejo, F.; Bandarenka, A.S. Nature of Highly Active Electrocatalytic Sites for the Hydrogen Evolution Reaction at Pt Electrodes in Acidic Media. *ACS Omega* **2017**, *2*, 8141–8147. [CrossRef] [PubMed]
26. Mahapatra, S.S.; Datta, J. Characterization of Pt-Pd/C Electrocatalyst for Methanol Oxidation in Alkaline Medium. *Int. J. Electrochem.* **2011**, *2011*, 563495. [CrossRef]
27. Gao, L.; Bao, Y.; Gan, S.; Sun, Z.; Song, Z.; Han, D.; Li, F.; Niu, L. Hierarchical Ni-Co Based Transition Metal Oxide Catalysts for Electrochemical Conversion of Biomass into Valuable Chemicals. *ChemSusChem* **2018**, *11*, 2547–2553. [CrossRef] [PubMed]
28. Ajeel, M.A.; Aroua, M.K.T.; Daud, W.M.A.W. Reactivity of carbon black diamond electrode during the electro-oxidation of Remazol Brilliant Blue R. *RSC Adv.* **2016**, *6*, 3690–3699. [CrossRef]
29. Choi, H.-J.; Jung, S.-M.; Seo, J.-M.; Chang, D.W.; Dai, L.; Baek, J.-B. Graphene for energy conversion and storage in fuel cells and supercapacitors. *Nano Energy* **2012**, *1*, 534–555. [CrossRef]
30. Nguyen, T.G.H.; Pham, T.V.A.; Phuong, T.X.; Lam, T.X.B.; Nguyen, T.P.T. Nano-Pt/C electrocatalysts: Synthesis and activity for alcohol oxidation. *Adv. Nat. Sci. Nanosci. Nanotechnol.* **2013**, *4*, 035008. [CrossRef]
31. Fashedemia, O.O.; Ozoemena, K.I. Enhanced methanol oxidation and oxygen reduction reactions on palladium-decorated FeCo@Fe/C core–shell nanocatalysts in alkaline medium. *Phys. Chem. Chem. Phys.* **2013**, *15*, 20982–20991. [CrossRef]

32. Meng, H.; Zeng, D.; Xie, F. Recent Development of Pd-Based Electrocatalysts for Proton Exchange Membrane Fuel Cells. *Catalysts* **2015**, *5*, 1221–1274. [CrossRef]
33. Larsen, R.; Ha, S.; Zakzeski, J.; Masel, R.I. Unusually active palladium-based catalysts for the electrooxidation of formic acid. *J. Power Sources* **2006**, *157*, 78–84. [CrossRef]
34. Liu, Q.; Liu, M.; Li, Q.; Xu, Q. Preparation and Electrocatalytic Characteristics of PdW/C Catalyst for Ethanol Oxidation. *Catalysts* **2015**, *5*, 1068–1078. [CrossRef]
35. Jiang, L.; Zhang, G.; Li, D.; Liu, C.; Xing, S. One-pot achievement of MnO_2/Fe_2O_3 nanocomposites for oxygen reduction reaction with enhanced catalytic activity. *New J. Chem.* **2019**, *43*, 16870–16875. [CrossRef]